Analyse des ESD-Verhaltens von Keramikvielschicht-Kondensatoren zur Bewertung der Festigkeit im Systemverbund

Stanislav Scheier [1], Stephan Frei [1]

(1) Technische Universität Dortmund, AG Bordsysteme, Friedrich-Wöhler-Weg 4, 44227 Dortmund

Zusammenfassung – Filternetzwerke bestehend aus einem Keramikvielschicht-Kondensator (engl. MLCC) teilweise ergänzt mit einem Widerstand sind eine verbreitete off-chip ESD Schutzstrategie. Es ist allgemein bekannt, dass die Kapazität eines MLCCs mit steigender Spannung abnimmt. Darüber hinaus kann eine wiederholte Belastung mit ESD zu irreversiblen Parameterveränderungen oder sogar physikalischen Schäden am MLCC führen. Diese Effekte können eine nichtausreichende ESD-Festigkeit oder – noch kritischer – eine Fehlfunktion des zu schützenden Systems verursachen. In diesem Paper wird ein Verfahren zur Charakterisierung des ESD-Verhaltens von MLCCs und zur Quantifizierung von Degradationseffekten infolge von wiederholter Pulsbelastung vorgestellt. Ein Verhaltensmodel wurde erstellt und in verschiedenen Setups validiert.

Abstract – Filter networks consisting of a Multilayer Ceramic Capacitor (MLCC) and maybe a resistor are commonly used as off-chip ESD-protection. It is generally known that MLCCs lose their capacitance at higher voltages. Additionally, repeated exposure to ESD can cause irreversible parameter shifts or physical damage to MLCC. The consequences of these effects may cause insufficient ESD robustness or - more critical - result in a malfunction of the system to be protected. In this paper methods are proposed to characterize the behavior of MLCCs at higher voltages and to quantify the degradation due to pulse load. The measured parameters are used for an accurate high voltage capacitor model. The model was applied in different setups. Simulation results were compared to measurements in order to prove the proposed approach.

1 Introduction

Electrostatic discharges (ESD) are a serious threat in the automotive-, industry-, and consumer-electronics. A discharge current caused by a human or a tool may flow through a sensitive IC pin and cause damages to an IC.

To avoid ESD failures on system level in many cases protection strategies are applied. A simple method is to equip the PCB with discrete protection components. Frequency selective elements like a Multilayer Ceramic Capacitor (MLCC) sometimes combined with a resistor are a common off-chip ESD-protection strategy to avoid ESD-problems. Due to its low cost and suitability as EMI-protection the capacitors play a leading role compared to other ESD-protection elements like nonlinear special devices. When a resistor is connected in series to the IC pin, the discharge current can be limited further (Figure 1).

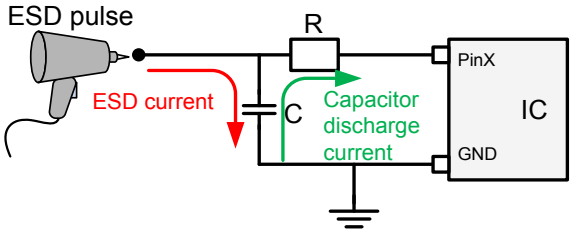

Figure 1: ESD protection by RC-filter.

Originally components like capacitors and resistors are not designed to protect against ESD. The majority of capacitors used on PCBs, have voltages rated between 50 V and 200 V. In case of ESD the capacitor has to stand voltages up to several kV and capacitors operate far above the absolute maximum ratings specified in datasheets.

It is generally known that MLCCs reduce their capacitance at higher voltages. It is not always possible to counteract this phenomenon by a MLCC of higher capacitance, because often the IC pins to be protected have to deal with high bitrate signals. A compromise is a lower capacitance which provides higher speed but less ESD protection. In [1] an improvement of the trade-off

using an antiferroelectric capacitor as ESD-protection is proposed. The dielectric constant of the hand-made capacitor increases with increasing voltage.

Repeated exposure to ESD can cause irreversible parameter shift on capacitors. The effects of derating on RF properties were investigated in [2]. A worst case out of four X7R 4.7 nF capacitors has shown a capacitance drop to 75 % of the nominal value, measured at 13.5 MHz. However, no modeling approaches for observed degradation effects were proposed. Physical damage to MLCCs exposed to ESD stress was examined by authors in [3] [4]. It was shown that ESD may cause a permanent damage to dielectric material. Significant differences in ESD performance of MLCCs from several manufacturers have been measured. The metallization of conductive plates within a capacitor results in a non-recoverable shift of insulation resistance of several MΩ to a lower value in the kΩ range. This will have an effect on the energy consumption of a system, and low current communication systems could be disturbed. The relationship between degradation of RF properties and damages on dielectric material is not analyzed yet.

PCB area consumption is an important criterion for the selection of protection elements. Technological progress enables smaller SMD package size whereas the capacitance and rated voltage remain the same. It is to be expected that this miniaturization will negatively affect the effects described above and a high voltage characterization method becomes more important.

A simulation of conditions to be expected on a PCB is an efficient solution to predict the system level ESD susceptibility. Anticipation of ESD failures requires exact models. A reliable model that combines the high voltage behavior of a MLCC in terms of capacitance drop, degradation effects and physical damages does not exist yet.

2 High Voltage Characterization

In order to characterize capacitors in the high voltage range special methods are necessary. Time- and frequency-domain analyses are possible. Here a time domain method is presented. The results shown here were measured with an arbitrary chosen 4.7 nF, 50 V 0603, X7R capacitor (Kemet C0603 C472K5RACTU).

2.1 Capacity

In MLCCs, ceramic material is acting as the dielectric. In order to increase the capacitance value using small package size, ceramics with high relative permittivity ε_r are used. It is obvious that the relative permittivity is not a constant value, but rather more a function of the applied voltage and frequency.

$$\varepsilon_r = f(V_{DC}, f) \tag{1}$$

Bariumtitanat (BaTiO3) is a ceramic material and most commonly used in X7R MLCCs. It is a ferroelectric, solid and belongs to the group of perovskite. According to additional additives and reduced fraction of BaTiO3 in MLCCs the ferroelectric properties of the ceramic are removed almost completely [2]. The spontaneous polarization is nearly zero and the ceramic may be approximated as paraelectric. The ESD frequency spectrum is significantly below 10 GHz. In that range BaTiO3 behaves like a dielectric with only orientation polarization and may be approximated as constant over frequency.

The capacitance for a linear capacitor is described by:

$$C = \frac{Q}{V} \tag{2}$$

For a nonlinear time independent capacitor the equation becomes:

$$C(V) = \frac{dQ}{dV} \tag{3}$$

It can be seen that the CV-curve is proportional to the derivative of the QV-curve. Consequently, both description options are qualitatively equivalent and may be used for high-voltage characterization of MLCCs.

A TLP can be used to measure the high voltage behavior of components in time domain [5]. The TLP creates a high voltage pulse. Some properties are comparable to real ESD events. Due to short pulse length, released energy is relatively low and device characterization for voltages far beyond the specification range is possible, without the risk of thermal damage. The setup in Figure 2 is adopted for MLCC characterization. When applying the TLP-pulse (HPPI- TLP/VF-TLP/HMM Test System TLP-3010C) to a DUT, voltage and current shapes are recorded by a 6 GHz oscilloscope (LeCroy WavePro 7 Zi) by voltage divider and a current sensor (Tektronik CT1) respectively. A source meter (Keithley 2400) is used to detect permanent damages on the insulation resistance after every TLP pulse. Any damage to the measuring instruments is avoided by attenuators.

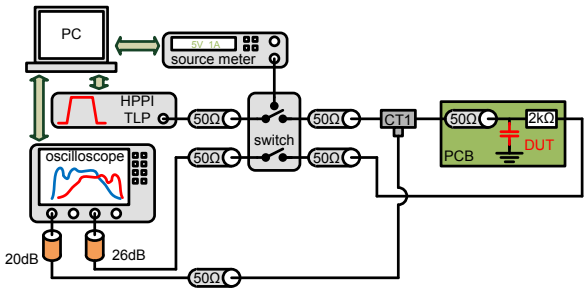

Figure 2: Measurement setup for MLCC characterization.

Several TLP pulses are applied to the MLCC, where the charging voltage is increased successively. To construct the QV-curve from TLP data a post-processing step is necessary. According to the definition, charge stored in the capacitor is equal to time integral over the current shape. This equation is applicable for both linear and nonlinear case.

$$Q = \int I dt \tag{4}$$

A cumulative integral function is used to obtain a charge over time curve. The voltage and charge values for a particular TLP charging voltage are detected in saturated state. Figure 3 illustrates measurement process described above.

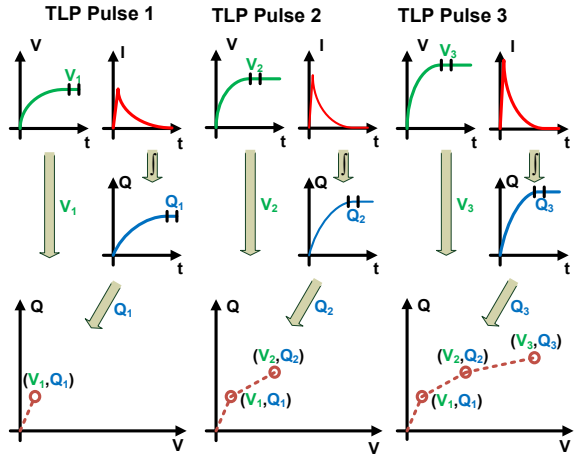

Figure 3: Measurement process for MLCC characterization by QV-curve with TLP. TLP charging voltage is increased from pulse 1 to pulse 3.

2.2 Approximation of QV-curve

Some simulation programs support a direct use of measured QV-curves, which may be implemented by a lookup table or an analytical approximating function. Others require a CV-curve, also known as the differentiated form of QV-curve. The discrete differentiation of the measured QV-curve will result in a noisy curve. A measured lookup table is not a continuous function and might lead to serious stability problems.

Approximation of the measured data by an analytical function is a better option. It reduces data noise. A continuously differentiable function is easier to handle by a simulation program and provides more stability. Most of the common simulation tools support so called equation defined blocks.

Hyperbolic tangent as a symmetric function is used to approximate the transition from the zero point to the saturated state [6]. When the ceramic is saturated, a linear behavior is expected.

$$Q = b_1 \tanh\left(\frac{V}{b_2}\right) + b_3 V \tag{5}$$

The derivative is:

$$C = \frac{dQ}{dV} = b_3 - \frac{b_1\left(\tanh^2\left(\frac{V}{b_2}\right)-1\right)}{b_2} \tag{6}$$

Figure 4 compares fitted and measured QV-curves. Figure 5 applies the fitted coefficients of the QV-curve to (6) and compares it with a discrete differentiated QV-curve. The tolerance within a set of MLCCs is presented too. The behavior of three samples is nearly the same. Damage on insulation resistance was measured between 900 V to 1000 V.

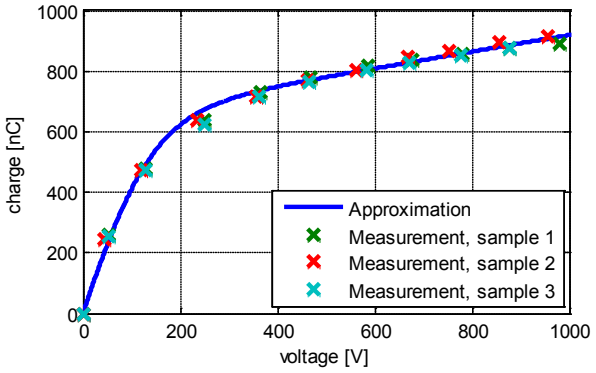

Figure 4: Measured and fitted QV-curve.

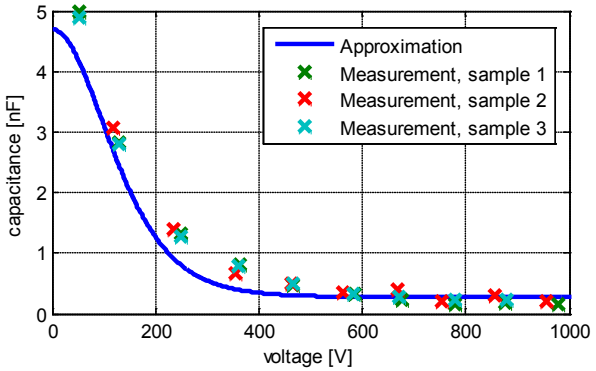

Figure 5: CV-curve applies the fitted coefficients of the QV-curve to (6).

2.3 Insulation breakdown

After a physical damage on insulation resistance has taken place, a change in leakage current of

more than a decade is observed. For the studied sample a critical voltage of 900 V can be measured (see Figure 6)

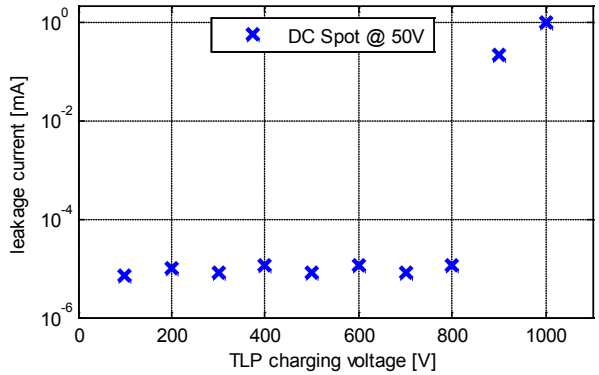

Figure 6: DC spots of the leakage current.

Voltage curves of a measurement with TLP pulses for an increasing charging voltage are shown in Figure 7. Only a single pulse was assigned for every voltage level. The MLCC withstands 800 V TLP pulse. 900 V is the critical voltage for insulation breakdown. This pulse cause damages and the voltage drops rapidly after 130 ns. Over the pre-damaged MLCC a 1000 V pulse is applied. At the beginning no changes in MLCC behavior can be observed. However, the critical voltage of the pre-damaged MLCC is considerably lower than the voltage of the faultless one. These results clearly state that the voltage on a MLCC is the critical parameter for the first failure.

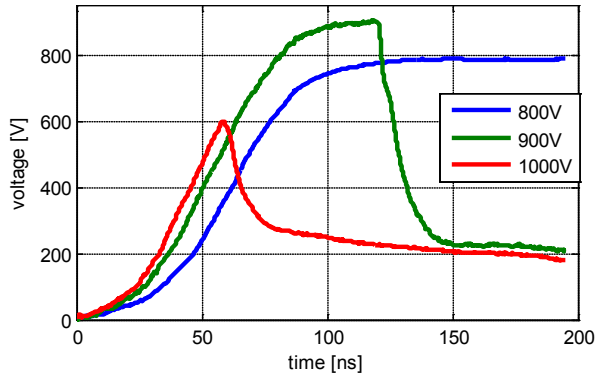

Figure 7: Measured voltage shapes. Low pass filtering is used for noise reduction.

Figure 8 shows the impedance analyzer measurement of the MLCC. The damaged device shows similar frequency response like the faultless one. The difference is caused by the change of the insulation resistance, where a drop from around 1 MΩ to 3.5 kΩ is measured. Capacity measurement at 13.5 MHz results in 4.42 nF for the faultless and 4.13 nF for the damaged MLCC. This means 7 % degradation in RF properties. In addition, Figure 8 provides a measurement, where the damaged capacitor was analyzed with a 30 V DC-offset. This condition leads to an Electrical Overstress (EOS) failure of the capacitor, where it becomes permanently conducting. Capacitive behavior cannot be seen any more and a short circuit of less than 1 Ω is measured.

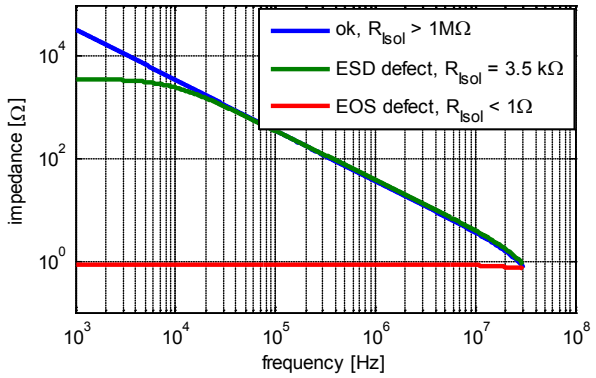

Figure 8: Impedance analyser measurement of a non-damaged MLCC, a MLCC after ESD failure, and an ESD-damaged MLCC after an EOS failure.

2.4 Degradation

In this section degradation effects on MLCC are analyzed. In particular low voltage capacitance and damages on dielectric material as a result of repeated ESD stress were measured. In previous section it was shown, that the applied voltage is crucial for insulation breakdown. Thus questions arise whether repeated stress at lower voltage level can cause permanent damage on insulation and, to what extent those damages are the reason for degradation of capacitance.

As already shown, TLP pulses of 900 V to 1000 V are critical for the investigated MLCC. The effects were examined in two test series, by 700 V as a high, but assumed to be safe voltage and by 1000 V as a critical voltage. Measurement process is illustrated in Figure 9. It is carried out by repetition of the following three steps:

1. High voltage stress: The MLCC is stressed by a certain number of TLP pulses of 200 ns length and 1.1 ns rise time. A permanently connected parallel 220 kΩ resistor is used to discharge the capacitor. No kind of degradation was measured on resistor.
2. Measurement of RF properties: impedance of MLCC is measured with vector network analyzer (VNA, Agilent E5061B) in frequency domain. Before measurement, VNA is calibrated and cables connecting the test PCB are de-embedded. Measurement range is between 1 kHz and 1 GHz.
3. Measurement of insulation resistance: a source meter (Keithley 2400) is used to detect permanent damages on insulation. Current

range (10 pA-1.05 A) is much higher in comparison to VNA. Voltage sweep is performed from 1 V to 50 V. Maximum source current is limited to 10 mA, to prevent damages.

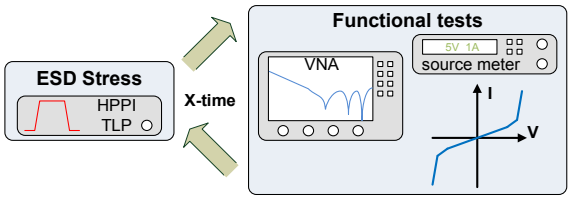

Figure 9: Measurement process for degradation characterization.

For parameter extraction measured impedance, after certain number of pulses, was approximated by model in Figure 13. The parameter R_{isol} was set to the corresponding result by source meter at 1 V. The parameters C, R_{ESR}, L_{ESL} were tuned to match with the measured impedance.

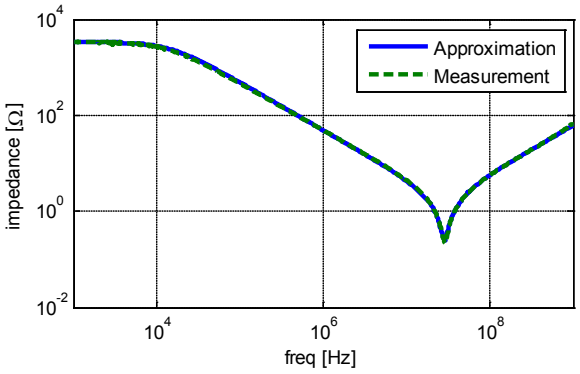

Figure 10: Approximation of the measurement after 1000 TLP pulses with 1000 V. C=3.22 nF, L_{ESL}=9.6 nH, R_{ESR}=240 mΩ, and R_{isol}=3.3kΩ.

Figure 11 and Figure 12 demonstrate the degradation results. For 700 V test series low voltage capacitance is decreasing strictly monotonic with additional pulses. For that effect some ferroelectric properties of the ceramic material may be responsible. Exposure of MLCC to voltages far beyond maximum ratings may lead to an asymmetrical shift in the equilibrium ion positions. This may cause a permanent dipole moment and hence a non-zero remanent polarization. Electric fields at normal operation are not strong enough to reverse that effect. However, no change in insulation resistance is visible. That means the degradation affects only the low voltage part of the QV-curve (5) and the ESD robustness of the MLCC remains quasi static.

As expected, insulation breakdown is observed after 10 pulses by 1000 V test series. As a result of metallization of conductive plates within the MLCC, insulation resistance falls by more than a decade. In general it continues to fall with additional high voltage pulses. However, the process does not behave consistently. The low voltage capacitive properties are affected by the mentioned process and the remanent polarization of the ceramic itself. After 3000 pulses a short of about 1 Ω is observed. No capacitive property can be measured anymore. In both test series no significant change in R_{ESR} and L_{ESL} was measured. Table 1 summarizes the degradation effects.

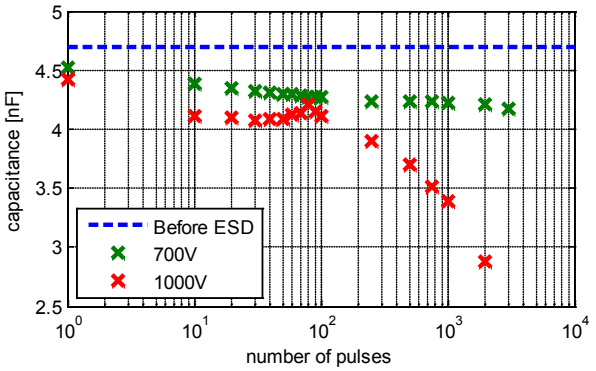

Figure 11: Degradation of capacitance. The results are normalized to 4.7 nF as initial value of every MLCC.

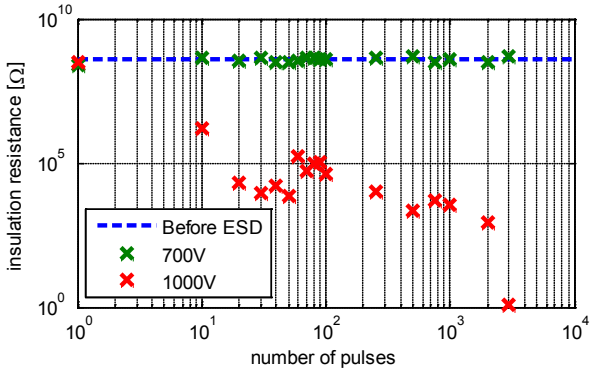

Figure 12: Degradation of insulation resistance.

Table 1: Parameter degradation of MLCC, Capacitance is normalized to 4.7 nF as initial value of every MLCC.

TLP Voltage	**C@ 0**	**C@ 1000**	**C@ 3000**	**R_{isol}@ 0**	**R_{isol}@ 1000**	**R_{isol}@ 3000**
700 V	4.7 nF (100 %)	4.21 nF (89 %)	4.17 nF (88 %)	>1 MΩ (100 %)	>1 MΩ (100 %)	>1 MΩ (100 %)
1000 V	4.7 nF (100 %)	3.38 nF (71 %)	NaN (≪1 %)	>1 MΩ (100 %)	3.3 kΩ (≪1 %)	≈1 Ω (≪1%)

2.5 Frequency domain behavior

The equivalent serial resistance and serial inductance are measured with an impedance analyzer. The process is the same as the measurement of RF properties during degradation analysis.

3 Modeling of MLCC in VHDL-AMS

An equivalent circuit of the MLCC is shown in Figure 13. Here the nominal capacitance is a function of the applied voltage; it is equivalent to the CV-curve in (6). According to the results in section 2.4, high voltage part of the QV-curve is not suffering from degradation. In case of undamaged dielectric, decrease in the capacitance is more significant at 100 V (Figure 5) than degradation effects. Right after the first failure of dielectric a proper function of MLCC may not be guaranteed anymore, even some additional ESD may shorten the circuit. Insulation resistance R_{isol} takes permanent ESD damages into account. The capacitor is assumed to be damaged, if the critical voltage was exceeded once. Parasitic elements R_{ESR} and L_{ESL} are included to represent frequency behavior.

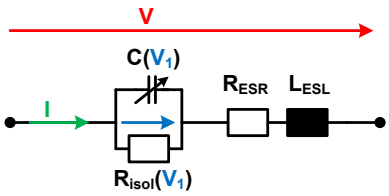

Figure 13: Advanced equivalent circuit of a MLCC.

4 Simulation Results

The setup in Figure 2 is simulated in VHDL-AMS. The model for TLP generator has been presented and verified by measurement with different low and high-ohmic loads in [7]. Figure 14 and Figure 15 compare simulated and measured curves for an 800 V TLP pulse. Absolute maximum ratings are violated and as a result, saturation may be observed. The transition to steady state is almost perfectly reproduced. The current maintains above zero, because of the parallel resistor of 2050 Ω. Low pass filtering of measurement data is applied for noise reduction.

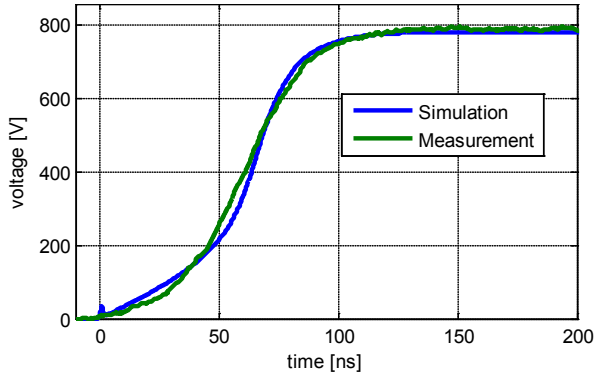

Figure 14: Simulated and measured voltage for 800 V TLP pulse.

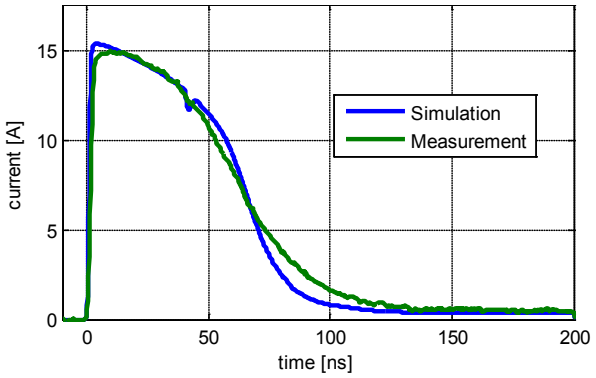

Figure 15: Simulated and measured current for 800 V TLP pulse.

An additional verification is done by means of an IEC-ESD-Generator. The model for a NoiseKen generator has been presented and verified by measurements with different low and high-ohmic loads in [8]. The NoiseKen generator is compliant to the IEC 61000-4-2 standard. MLCC acting as ESD protection element is loaded with IEC ESD pulses. The setup shown in Figure 16 is used. ESD current is measured with a Tektronix CT1 current probe. A parallel 10 kΩ resistor is used to provide a discharge load. Additionally, it provides a discharge path for MLCC between consecutive IEC-pulses and ensures proper initial conditions of MLCC. The ESD current is measured only. A simulation of an ideal 4.7 nF capacitor is included to highlight the extent of nonlinearity for real MLCC.

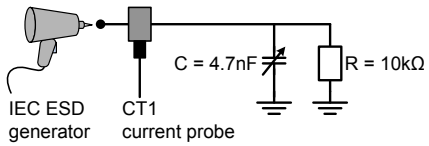

Figure 16: Measurement and simulation setup for IEC ESD pulses.

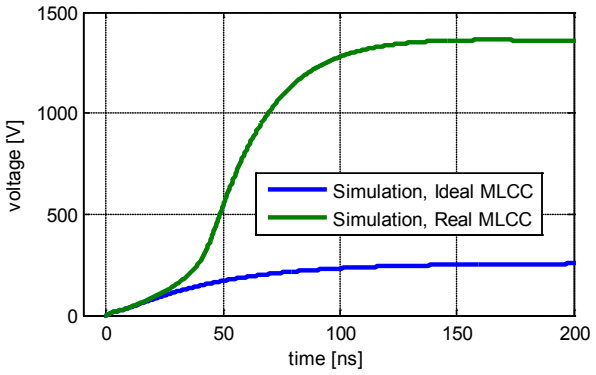

Figure 17: Simulated voltage for 8 kV IEC ESD pulse.

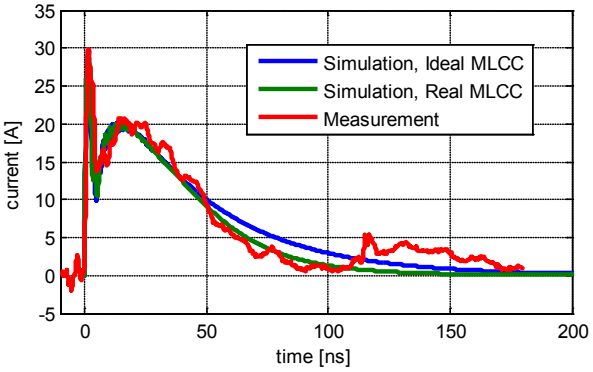

Figure 18: Simulated and measured current for 8 kV IEC ESD pulse.

Simulation shows an insulation breakdown at 63.8 ns. In measurement a MLCC failure is observed at about 100 ns. The MLCC becomes conductive and a rise in ESD current is measured. After the ESD stress, an isolation resistance of 8 kΩ is measured. There is a significant difference in voltage level on real and ideal MLCC. This result highlights the need of an accurate MLCC model with regard to transient high voltage behavior for reliable ESD simulation.

5 Conclusion

A method to characterize the transient high voltage behavior of MLCC is proposed and successfully applied to a test capacitor. Before insulation breakdown takes place, only the low voltage capacitance is suffering from degradation but ESD protective properties remain the same as before. It is shown that applied voltage is the crucial parameter that may cause insulation breakdown. A pre-damaged MLCC is more susceptible to electrical overstress. A destructive current can be triggered within absolute maximum ratings. This will have a major effect on the energy consumption of a system and high impedance communication could be disturbed.

A model for a MLCC is implemented in VHDL-AMS and validated for different ESD-pulses. With the accurate MLCC model a simulation based prediction of ESD failures is possible. When a MLCC is used as an ESD protection element, its high voltage behavior has to be considered, in order to reach reliable protection and to avoid functional failures.

Acknowledgement

The reported R+D work was carried out within the CATRENE project CA310 EM4EM (Electromagnetic Reliability and Electronic Systems for Electro Mobility). This particular research is supported by the BMBF (Bundesministerium fuer Bildung und Forschung) of the Federal Republic of Germany under grant 16 M3092 I. The responsibility for this publication is held by the authors only.

References

[1] Hongyu Li; Khilkevich, V.; Tianqi Li; Pommerenke, D.; Seongtae Kwon; Hackenberger, W.; , "Nonlinear capacitors for ESD protection," Electromagnetic Compatibility Magazine, IEEE , 2012

[2] Streibl, F.; "Electrostatic Discharge Performance of Passive Surface-Mount Components,", 2011 Books on Demand GmbH, ISBN 978-3-84236-670-1

[3] Rostamzadeh, C.; Dadgostar, H.; Canavero, F.; , "Electrostatic Discharge analysis of Multi Layer Ceramic capacitors," Electromagnetic Compatibility, EMC 2009. Aug. 2009

[4] Demcko, R.; Ward, B.; , "MLCC ESD characterization," CARTS 2007 Symposium Proceedings, Albuquerque, Mar. 2007

[5] Simbuerger, W.; Johnsson, D.; Stecher, M.; , "High Current TLP Characterisation: An Effective Tool for the Development of Semiconductor Devices and ESD Protection Solutions," ARMMS RF & Microwave Society, 2012

[6] Manly, W., Jr.; , "An appraisal of several nonlinear hysteresis loop models," Magnetics, IEEE Transactions, 1973

[7] Cao, Y.; Arndt, B.; zur Nieden, F.; Stecher, M.; Frei, S.; „Charakterisierung und systematische Bewertung von externen ESD Schutzelementen," EMV Düsseldorf, 2010

[8] Zur Nieden, F.; Arndt, B.; Kremer, F.; Cao, Y.; Edenhofer, J.; Frei, S.; „Vergleichbarkeit von ESD-Prüfungen auf IC- und Systemebene oder welchen Einfluss hat eine Reduzierung der IC-ESD-Festigkeit auf die Systemfestigkeit?" EMV Düsseldorf, 2010